

Assessing the performance of exchange-correlation functionals on lattice constants of binary solids at room temperature within the quasiharmonic approximation

Xiaofei Shao,¹ Peitao Liu ², Cesare Franchini,^{3,4} Yi Xia,⁵ and Jiangang He ^{1,*}

¹*School of Mathematics and Physics, University of Science and Technology Beijing, Beijing 100083, China*

²*Shenyang National Laboratory for Materials Science, Institute of Metal Research, Chinese Academy of Sciences, 110016 Shenyang, China*

³*University of Vienna, Faculty of Physics and Center for Computational Materials Science, 1090 Vienna, Austria*

⁴*Department of Physics and Astronomy “Augusto Righi”, Alma Mater Studiorum, Università di Bologna, 40127 Bologna, Italy*

⁵*Department of Mechanical and Materials Engineering, Portland State University, Portland, Oregon 97201, USA*



(Received 30 April 2023; accepted 6 July 2023; published 20 July 2023)

The exchange-correlation functional is at the core of density functional theory (DFT) and determines the accuracy of DFT in describing the interactions among electrons/ions in solids and molecules. The strongly constrained and appropriately normed functional (SCAN) and its derivatives, regularized SCAN (rSCAN) and regularized-restored SCAN (r²SCAN), are particularly promising due to their remarkable overall accuracy in the description of various properties while retaining a high computational efficiency as compared to hybrid functionals. However, an exhaustive assessment on the performance of these functionals in predicting the finite-temperature lattice constant of solids is still lacking. Here, we systematically study the room-temperature lattice constants of 60 cubic binary compounds within the quasiharmonic approximation using SCAN, rSCAN, r²SCAN, local density approximation (LDA), and two common generalized gradient approximation (GGA) functionals, Perdew-Burke-Ernzerhof (PBE) and revised PBE for solid and surface (PBEsol). We found that SCAN exhibits numerical instabilities in free energy calculations, manifested by the presence of spurious imaginary frequencies in phonon dispersion relationships and poor fitting in Murnaghan’s equation of state of Helmholtz free energy for 30 compounds. The revised SCAN functionals show much better numerical stabilities and reduce the number of the compounds with numerical issues to 22 and 9 for rSCAN and r²SCAN, respectively. The mean relative absolute errors (MRAE) of the calculated lattice constants at room temperature for the remaining 30 binary compounds are 0.92%, 1.10%, 0.32%, 0.51%, 0.58%, and 0.67% for LDA, PBE, PBEsol, SCAN, rSCAN, and r²SCAN, respectively. Furthermore, we found that the SCAN functional incorrectly predicts unstable phonon modes for a few compounds at their equilibrium volumes, which indicates the existence of a new ground state structure with lower energy than the cubic structure at 0 K, disagreeing with experiments. Our results provide a useful guide in choosing suitable functionals in describing anharmonic phonons and shed light on second-order force constant calculations that may help to develop more accurate exchange-correlation functionals for solids.

DOI: [10.1103/PhysRevB.108.024306](https://doi.org/10.1103/PhysRevB.108.024306)

I. INTRODUCTION

One of the most attractive features of density functional theory (DFT) is its capability to accurately obtain the energies and forces of a given structure for solids and molecules at a moderate computational cost. The quick prevalence of DFT in condensed matter physics, computational chemistry, and material science benefits from simple but relatively accurate local and semilocal exchange-correlation functionals: local density approximation (LDA) and generalized gradient approximation (GGA) [1–3]. Improvements have been made by adding more terms in exchange and correlation parts towards a higher rung of Jacob’s ladder [4], such as meta-GGA [5–7], hybrid functionals [8–11], and double hybrid functionals [12]. Although LDA [13], Perdew-Burke-Ernzerhof (PBE) [3], revised PBE for solid and surface (PBEsol) [14], and Heyd-Scuzeria-Ernzerhof (HSE06) [15] are the most

popular functionals in the solid-state community, none of these functionals are capable of describing well all the systems and properties. For example, LDA generally performs well for homogeneous electron systems, while PBEsol is optimized for solid and surface and can capture a certain amount of van der Waals correction [16]. The strongly constrained and appropriately normed meta-GGA functional (SCAN), which was developed in 2015 by Sun *et al.* [17], obeys all 17 known exact constraints [18–20]. The initial tests show that SCAN works well for systems from weakly bonded molecules to strongly correlated oxides and describes much better lattice constants, cohesive energies, and bulk moduli than the PBE and a few other functionals commonly used in solids [17–21]. Recently, however, SCAN was found to be less accurate for the formation energies of weakly bounded intermetallic compounds than PBE, although it significantly improves those for strongly bound compounds such as oxides [22]. The performance of SCAN in describing the magnetic properties of transition metals is found to be problematic as well [20,23]. Charles and Rondinelli studied the structural, electronic, and

*jghe2021@ustb.edu.cn

lattice dynamical properties of 19 oxyfluoride compounds using LDA, GGA, meta-GGA, and hybrid functionals, and found that SCAN is more accurate than LDA and PBE, but not better than PBEsol and hybrid functionals [24]. In addition, SCAN suffers numerical instability, which needs a denser fast Fourier transform (FFT) grid and may cause divergence in self-consistent calculations in some cases [25,26]. To mitigate the numerical issue of SCAN, the regularized form of the SCAN functional (rSCAN) was proposed but at the cost of breaking some constraints [25]. However, it was found that rSCAN exhibits larger errors than SCAN in certain systems [27,28]. To compromise the accuracy and efficiency, the regularized-restored SCAN functional (r²SCAN) was recently developed [26]. Recently, Kingsbury *et al.* found that r²SCAN predicts formation energies more accurately than SCAN and PBEsol for both strongly and weakly bound materials, and that r²SCAN predicts systematically larger lattice constants than SCAN [29]. Nevertheless, the performances of rSCAN and r²SCAN on many other properties have not yet been thoroughly tested yet.

The lattice constant is a fundamental property of solids, and therefore its accurate description is always utilized to assess new functionals [17,18,25,26]. However, a direct comparison between experimental lattice constants (usually measured at room temperature) and the DFT calculated ones at 0 K is deceptive because of the zero point vibration and thermal expansion stemming from the lattice anharmonic effects. Since the accurate calculation of lattice constants at room temperature involves computing higher-order force constants that demand high computational resources, the primary approach in the literature is to extrapolate the measured lattice constants at room temperature to 0 K by assuming a linear thermal expansion and subtracting the zero point anharmonic expansion (ZPAE) [30–37], using either a semiempirical formula based on the Debye model [33,34] or the calculated zero point energy (ZPE) from phonons within the quasiharmonic approximation (QHA) [35–37]. A rather large error can be induced by the assumptions of a linear expansion from 0 K to room temperature and the Debye model, which does not include the optical phonon modes. Moreover, this approach cannot assess the performance of a functional on the anharmonic effect of crystals at finite temperatures, which is, however, important for computing the lattice thermal expansion coefficient, phonon transport, and other temperature-dependent properties. The assessment of different exchange-correlation functionals on anharmonicity has not been systematically studied. In particular, the performance of functionals in computing high-order force constants is unclear, leading to large discrepancies in the literature. For example, Xia *et al.* studied lattice thermal conductivities of Ti_3VSe_4 using PBEsol [38], while Jain performed similar calculations for this compound using PBE [39]. However, they obtained different conclusions on the origin of the low lattice thermal conductivity in Ti_3VSe_4 [38,39]. Oba *et al.* studied the thermal expansion of ScF_3 within quartic anharmonicity, and found that LDA is better than PBE and PBEsol in reproducing the thermal expansion coefficient in a wide temperature range [40]. Bichelmaier *et al.* obtained a good agreement between the calculated thermal expansion coefficient of Hafnia and experimental value using PBE functional [41]. Amano *et al.*

studied lattice dynamics of TiO_2 using the r²SCAN functional, showing a good agreement between calculated lattice constants and phonon spectrum and experimental data [42]. Furthermore, the corrections coming from different approximations in dealing with anharmonic effects complicate the assessment of the functionals.

QHA is often used as a practical approach to study lattice constants at finite temperatures [43], which allows a direct comparison with experimental lattice constants, and therefore enables us to assess the performance of different functionals at finite temperatures directly. Although QHA is a first-order approximation for dealing with anharmonicity, it is accurate enough for compounds with weak anharmonicity or at low temperatures, e.g., room temperature. In the literature, QHA has been widely employed to study the thermal expansion of solids at relatively low temperatures [44–50]. For example, Skelton *et al.* evaluated the performance of LDA, GGA, and meta-GGA functionals on lattice dynamics of four binary semiconductors (PbS, PbTe, ZnS, and ZnTe) within QHA, though PbS and PbTe are well known materials for their strong anharmonicity [44]. They found that PBEsol shows the best performance among all the tested functionals. Previous studies on the negative thermal expansion of Cu_2O within QHA found good agreement between experiments and calculations at room temperature [45,46]. However, one should note that phonons at finite temperature are renormalized, and such effects are more pronounced when the lattice is quite anharmonic or at high temperatures. QHA may predict unphysical phonon behaviors when anharmonicity is very strong. In this scenario, it is difficult to assess a functional's performance due to error cancellation. Therefore, in this work we avoided the compounds with strong anharmonicity.

In this work, we systematically assess the performance of three widely used functionals in solids (LDA, PBE, and PBEsol) and three SCAN-based functionals (SCAN, rSCAN, and r²SCAN) on the description of the lattice constants of 60 binary compounds with four different structure types at room temperature. We find that SCAN has serious numerical instability, leading to spurious imaginary phonon frequencies at extended/compressed volumes and poor fitting of the equation of state for 30 compounds that impede their lattice constant calculations at room temperature. Both rSCAN and r²SCAN demonstrate better numerical stabilities than SCAN. PBEsol exhibits the smallest MRAE for the lattice constants at room temperature among all the considered functionals, which is followed in a decreasing sequence by SCAN, rSCAN, r²SCAN, LDA, and PBE.

II. METHODS

All first-principles calculations were performed using the projector augmented wave (PAW) pseudopotential method [51,52], as implemented in the Vienna *Ab initio* Simulation Package (VASP) [53,54]. Except for LDA, we used the PBE-version PAW pseudopotential for all the other functionals. Although this could lead to certain errors in SCAN, rSCAN, and r²SCAN due to the lack of compatible SCAN PAW pseudopotential in VASP, almost all previous studies for solids used the PBE pseudopotential, and negligible errors were found [18,23,27]. The plane wave basis set with an

energy cutoff of 520 eV was used for all the functionals except SCAN, rSCAN, and r^2 SCAN, where a much larger energy cutoff of 800 eV was used. In addition, for SCAN, rSCAN, and r^2 SCAN, the precision parameter was set to “accurate” (PREC=ACCURATE), nonspherical contributions within the PAW spheres were included (LASPH=TRUE.), and additional grids for the evaluation of the augmentation charges (ADDGRID=TRUE.) were adopted. The Γ -centered Monkhorst-Pack k -point grid of KPPRA (k points per reciprocal atom) ≈ 10000 was used to sample the first Brillouin zone for all the functionals. Crystal structures were fully relaxed until the Hellmann-Feynman forces acting on each atom were less than 0.01 eV/Å.

The lattice constants at room temperature were calculated within QHA. For each compound, the phonons were computed at 11 different volumes spanning from -10% to 10% of the equilibrium volume at 0 K. The equilibrium volume at 300 K was obtained by fitting the volume-dependent Helmholtz free energy using the Murnaghan equation of state [55]. The second-order force constants at each volume were computed using the finite displacement method with a $4 \times 4 \times 4$ (128 atoms for rocksalt, zinc-blende, and cesium chloride structures; 192 atoms for fluorite structure) supercell of the primitive unit cell and displacement of 0.01 Å. The random phase approximation (RPA) [56,57], which is an accurate many-body theory and often used to benchmark other functionals [16,58–61], was used to calculate the Γ_4^- phonon mode of PbTe. The anharmonic phonon renormalization of PbTe at 0.1 K is carried out by means of self-consistent phonon theory (SCPH) formulated in the reciprocal space with $4 \times 4 \times 4$ supercells; see Ref. [38] for more details.

III. RESULTS AND DISCUSSIONS

In this work, 60 binary compounds, including 30 rocksalt (space group $Fm\bar{3}m$), 22 zinc blende (space group $F\bar{4}3m$), 4 cesium chloride (space group $Pm\bar{3}m$), and 4 fluorite ($Fm\bar{3}m$), are studied within QHA (see the list of compounds in Table S1 of the Supplemental Material [62]). We found 5, 2, 4, 28, 14, and 12 of them have imaginary phonon frequencies in at least one of the 11 volumes for the calculations conducted by LDA, PBE, PBEsol, SCAN, rSCAN, and r^2 SCAN functionals, respectively. All of the imaginary frequencies appearing in LDA, PBE, and PBEsol are due to the overextended ($\sim 10\%$) or overcompressed ($\sim -10\%$) volume, and these imaginary frequencies are associated with distorted structures that have lower energies than the structure performing phonon calculations. Since the presence of imaginary frequencies impedes the calculation of vibrational entropy and ZPE, we eliminated the volumes with imaginary frequencies and performed the EOS fitting for the rest of the volumes. We also checked the quality of EOS fitting by monitoring the R^2 (R -squared) value and only the fitting with R^2 higher than 0.995 were used for lattice constant calculations. The number of imaginary frequencies and the R^2 value of each compound for different functionals are tabulated in Tables S1 and S2 of the Supplemental Material (SM) [62], respectively. By contrast, most of the volumes with imaginary frequencies appearing in SCAN, rSCAN, and r^2 SCAN are due to numerical instabilities, and only a few of

them are caused by overcompressed/overexpanded volumes. Except for the observation of more volumes with imaginary frequencies in SCAN, rSCAN, and r^2 SCAN, we found that there are more compounds whose free energies calculated by SCAN cannot be fitted by the Murnaghan equation of state, even if the volumes with imaginary frequencies are eliminated, i.e., the R^2 of the EOS fitting is lower than 0.99; see Table S2 [62]. Therefore, only 30 compounds with good EOS fitting ($r^2 \geq 0.995$) remain for SCAN; see Table S2 [62]. The r^2 SCAN exhibits fewer compounds with imaginary frequencies and thus there are more compounds with good EOS fitting than SCAN and rSCAN (see Table S2 [62]), consistent with its design purpose for improving numerical stability [26].

A. Lattice constants with zero point energy correction

As mentioned above, the zero-point anharmonic correction has been widely used in lattice constants comparison between experiments and DFT calculations [31–37]. We first compare our results with the previous study by Zhang *et al.*, who assessed the performance of LDA, PBE, PBEsol, M06-L [63], SCAN, and HSE06 [64] on lattice constants of 64 solids using the ZPAE method, including metals and semiconductors of elemental bulks and binary compounds [37]. The ZPE correction was employed based on the DFT calculated phonons of each functional within QHA. The comparison with our results is shown in Fig. S1 [62]. Overall, our results of the lattice constant difference (Δa) with and without ZPE-correction agree very well with Zhang’s calculations for all four functionals (LDA, PBE, PBEsol, and SCAN) [37], though we used a larger ($4 \times 4 \times 4$) supercell and plane wave basis sets, while Zhang *et al.* used a $2 \times 2 \times 2$ supercell and numeric atom-centered orbital basis functions [37].

The Δa of 30 compounds calculated by six functionals in this work is shown in Fig. S2 [62]. Overall, the Δa calculated using different functionals are similar across these functionals, which agrees with the previous observation using PBE and LDA [35], where phonon calculations were only conducted using PBE and the same ZPE correction was applied to all the functionals. However, a few exceptions exist. For example, SCAN predicts that YN shows the smallest Δa among these compounds, but the other four functionals yield a relatively larger Δa . Similar observations are obtained in Δa of LaP calculated by PBEsol and BaSe by LDA. Therefore, it is necessary to carry out phonon calculations for each functional to impose correct ZPE correction.

The comparison of the ZPE-corrected lattice constant with all six functionals is shown in Fig. 1. Among these functionals, PBEsol has the smallest MRAE (0.39%) while PBE has the largest MRAE (1.14%) with all the lattice constants being overestimated. Three SCAN-related functionals have similar MRAE, and r^2 SCAN has the largest MRAE among them. A larger set of compounds, where SCAN and rSCAN calculations are excluded because of their numerical issue, is shown in Fig. S3 of the Supplemental Material [62]. The MRAEs are almost the same for PBE, PBEsol, and r^2 SCAN. However, the MRAE of LDA increases from 0.75% to 1.19% because there are more compounds with underestimated lattice constants by LDA. Therefore, LDA and PBE have very similar MRAE but

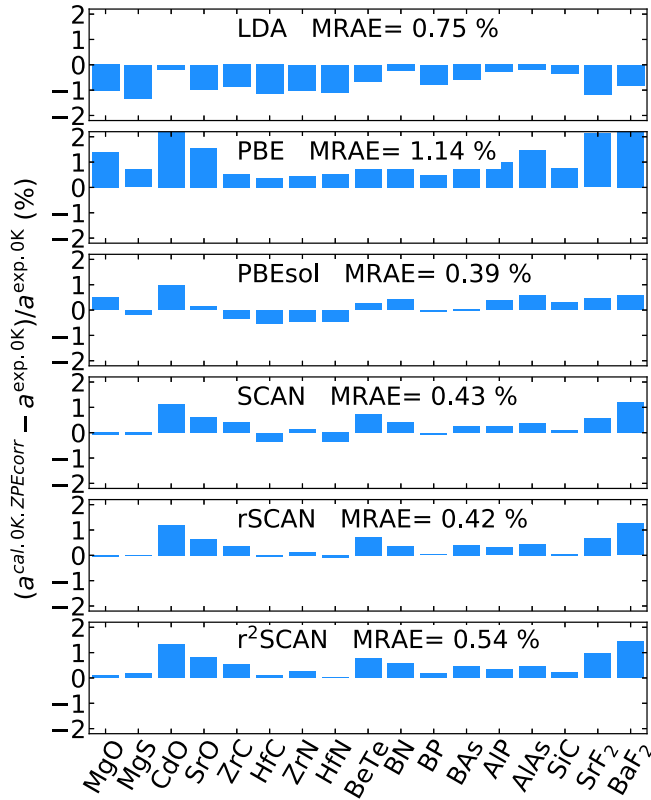


FIG. 1. Relative errors of DFT computed lattice constants including ZPE correction with respect to the experimental lattice constants extrapolated to 0 K.

very different trends of overestimation, which is similar to the previous study by Zhang *et al.* [37].

B. Lattice constants at room temperature

In this section, we perform a direct comparison between the calculated lattice constants at 300 K within QHA and experimental values measured at room temperature. The relative error (RE) of lattice constants is defined as $(a^{\text{cal.300K}} - a^{\text{exp.300K}})/a^{\text{exp.300K}}$, where $a^{\text{cal.300K}}$ and $a^{\text{exp.300K}}$ are the DFT calculated lattice constants at 300 K within QHA and experimental values measured at room temperature, respectively. As shown in Fig. 2, PBEsol exhibits overall the smallest RE among all these six functionals, with the largest RE less than $\pm 1.00\%$. Both PBE and r^2 SCAN overestimate the lattice constants of all the compounds, while LDA underestimates all the lattice constants. SCAN overestimates the lattice constants except for HfN, and rSCAN overestimates the lattice constants except for MgO. The MRAEs of the 30 compounds are 0.92%, 1.10%, 0.32%, 0.51%, 0.58%, and 0.67% for LDA, PBE, PBEsol, SCAN, rSCAN, and r^2 SCAN, respectively. Similarly to the case of ZPAE, PBEsol has the smallest MRAE and PBE has the largest MRAE among these functionals. Three SCAN-based functionals have very similar REs for each compound and r^2 SCAN has the largest MRAE due to the overestimation in many compounds, which is consistent with the results observed by Kingsbury *et al.* [29]. In the dataset with 53 compounds (see Fig. S4 [62]), the MRAEs of LDA, PBE, PBEsol, and r^2 SCAN are 1.01%, 1.30%, 0.39%, and 0.75%,

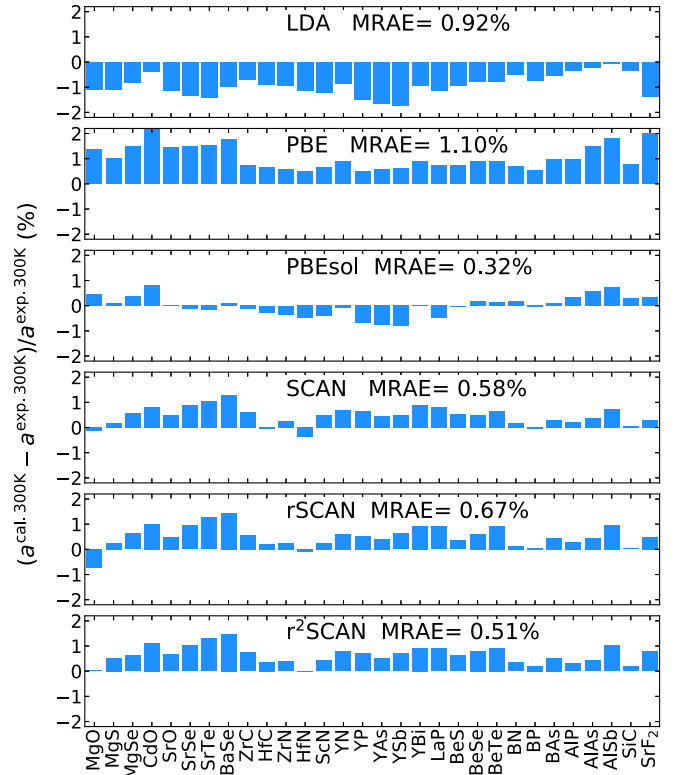


FIG. 2. Relative errors of DFT calculated lattice constants at 300 K within QHA with respect to the experimental values at room temperature.

respectively, which are close to the results of 30 compounds, suggesting a consistent MRAE of these functionals.

The reason that PBEsol has the smallest MRAE between the calculated lattice constants at room temperature and experimental values is due to the cancellation of slightly underestimated lattice constants at 0 K by PBEsol and increased lattice constants associated with the thermal expansion of these compounds at room temperature; see Fig. S5 [62]. Since the 0 K lattice constants calculated by SCAN, rSCAN, and r^2 SCAN are already slightly larger than the experimental lattice constants at room temperature for most compounds, the inclusion of thermal expansion would further enlarge the MRAEs. Similarly, the MRAE of LDA calculated at room temperature (0.92%) is alleviated as compared to its serious underestimation at 0 K (1.29%), while it is enhanced from 0.66% to 1.10% by PBE because of its overestimation at 0 K. Our results show that LDA underestimates but PBE overestimates all the studied lattice constants at room temperature, as expected from the standard LDA/PBE known trends. The consideration of thermal expansion improves the predictions of LDA but worsens those of PBE. The PBEsol functional exhibits the best performance on the lattice constants prediction, while the SCAN-based functionals tend to overestimate the lattice constants of the studied compounds.

C. Grüneisen parameter at room temperature

The Grüneisen parameter (γ), which is defined as the change of phonon frequency with respect to the variation of the unit cell volume, is often used to characterize the strength

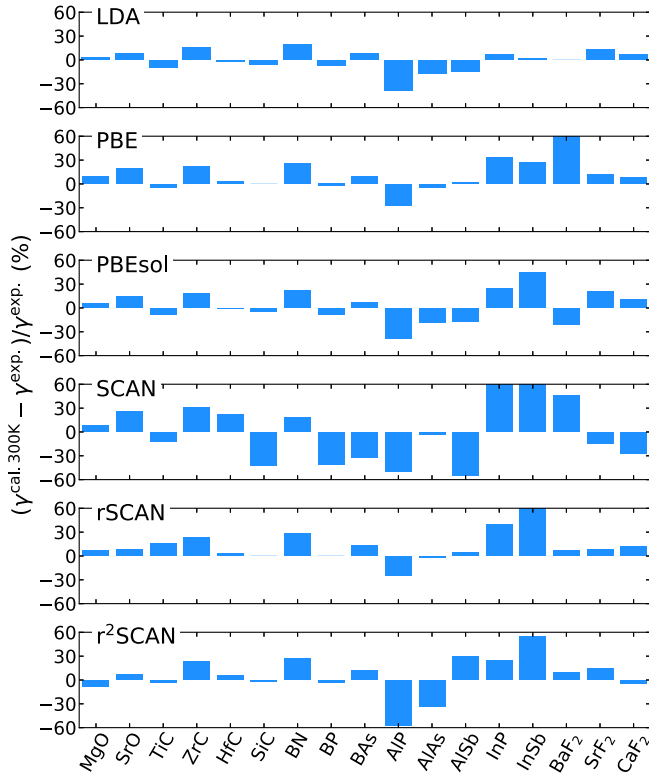


FIG. 3. The relative error of DFT Calculated Grüneisen parameters (γ) at 300 K with respect to experiment values.

of the anharmonic effect and calculate lattice thermal conductivity and thermal expansion coefficient [65–67]. Although γ is often calculated at 0 K in the literature, it is actually temperature dependent. In Fig. 3, we show the RE between the experimental γ and our calculated averaged Grüneisen parameter at 300 K using different functionals for 17 compounds whose experimental γ are available [68–70]. The MRAEs of LDA, PBE, PBEsol, SCAN, rSCAN, and r²SCAN are 10.5%, 15.9%, 16.6%, 41.8%, 31.9%, and 18.8%, respectively. The result is very different from the case of the lattice constant. LDA has the smallest MRAE, with the largest RE being -38.7% in AlP, which is still smaller than the MRAE of SCAN. The MRAE of r²SCAN is smaller than SCAN and rSCAN, but larger than LDA, PBE, and PBEsol. Our results indicate that the SCAN-based functionals might not be advantageous compared with other functionals in describing the anharmonic properties of solids. Note that thermal expansion calculated using QHA works well only for weak anharmonic crystals. For the compounds with strong anharmonicity, even if QHA predicts the thermal expansion correctly, the underlying physics regarding lattice dynamics can be completely off, e.g., QHA may predict opposite γ as compared to the experimental values.

D. Correlation between relative errors of lattice constants and properties of compounds

It is instructive to see how the REs of the lattice constants calculated at room temperature with respect to experimental values are correlated with the key properties of materials

such as formation energy (ΔH), bulk modulus (G), Grüneisen parameter (γ), and band gap (E_g). To this end, we present the correlation relationships for different functionals in Fig. 4. The formation energies of these compounds are taken from the Open Quantum Materials Database (OQMD) [71], whereas bulk modulus, Grüneisen parameters, and band gaps are calculated using PBEsol functional. The correlation between RE and formation energy is obvious in all these functionals except PBEsol: the compound with smaller formation energy generally has smaller RE. The REs of PBEsol are small and nearly independent of formation energy, with the largest RE being at $\Delta H \approx -1.0$ eV/atom. An inverse correlation is observed in bulk modulus for all these functionals, i.e., the compound with a large bulk modulus has a smaller RE. This is because the compound with large formation energy and bulk modulus generally has stronger chemical bonds, weaker anharmonicity, and smaller thermal expansion. The trend of RE is different from that of formation energy observed in SCAN [22], where the error of SCAN is smaller for the strongly bound compounds and larger for the weakly bound compounds, showing the difference between formation energy and anharmonicity. It is known that the zinc-blende structure usually has smaller γ than the rocksalt one, due to its lower coordination number and shorter bond lengths between cation and anion. The correlation between RE and γ is only apparent in LDA and PBE, where RE increases and decreases with γ increasing for LDA and PBE, respectively. This is unexpected because the underestimation of the lattice constant at 0 K by LDA should be better compensated by a larger thermal expansion at room temperature for the compounds with large γ (the linear expansion coefficient is usually proportional to γ), i.e., the calculated lattice constant at room temperature for the compound with large γ should be closer to the experimental value than the compound with smaller γ . The RE is nearly independent of γ for the other four functionals. Also, the dependence of RE on the band gap is not obvious for all these functionals, indicating a weak correlation with the electronic structures. All these trends are similar in the larger data set when SCAN calculations are excluded; see Fig. S6 of the SM [62].

E. Numerical instabilities of SCAN-related functionals

Within the studied 60 compounds, we found that 30 of them have the R^2 of free energy EOS fitting less than 0.995 (see Table S2 and Figs. S7 and S8 of the SM [62]). Note that, for the compounds having volumes with imaginary frequencies, we excluded these volumes and performed the fitting for the rest of the volumes. As observed in Table S1, SCAN and SCAN-related functionals tend to result in much more spurious imaginary frequencies in the volume range close to that of PBEsol. We also found that these spurious imaginary frequencies do not necessarily reduce total energy if their eigenvectors are condensed but might arise from the interpolation error when computing phonon dispersion via the Fourier transformation of force constants, which is different from the cases for LDA, PBE, and PBEsol. In addition, we found that despite the absence of imaginary frequencies, some compounds have poor fitting R^2 too, such as SrS, SnAs, and YBi. Both rSCAN and r²SCAN have better numerical stabilities than SCAN, especially for r²SCAN. The numbers

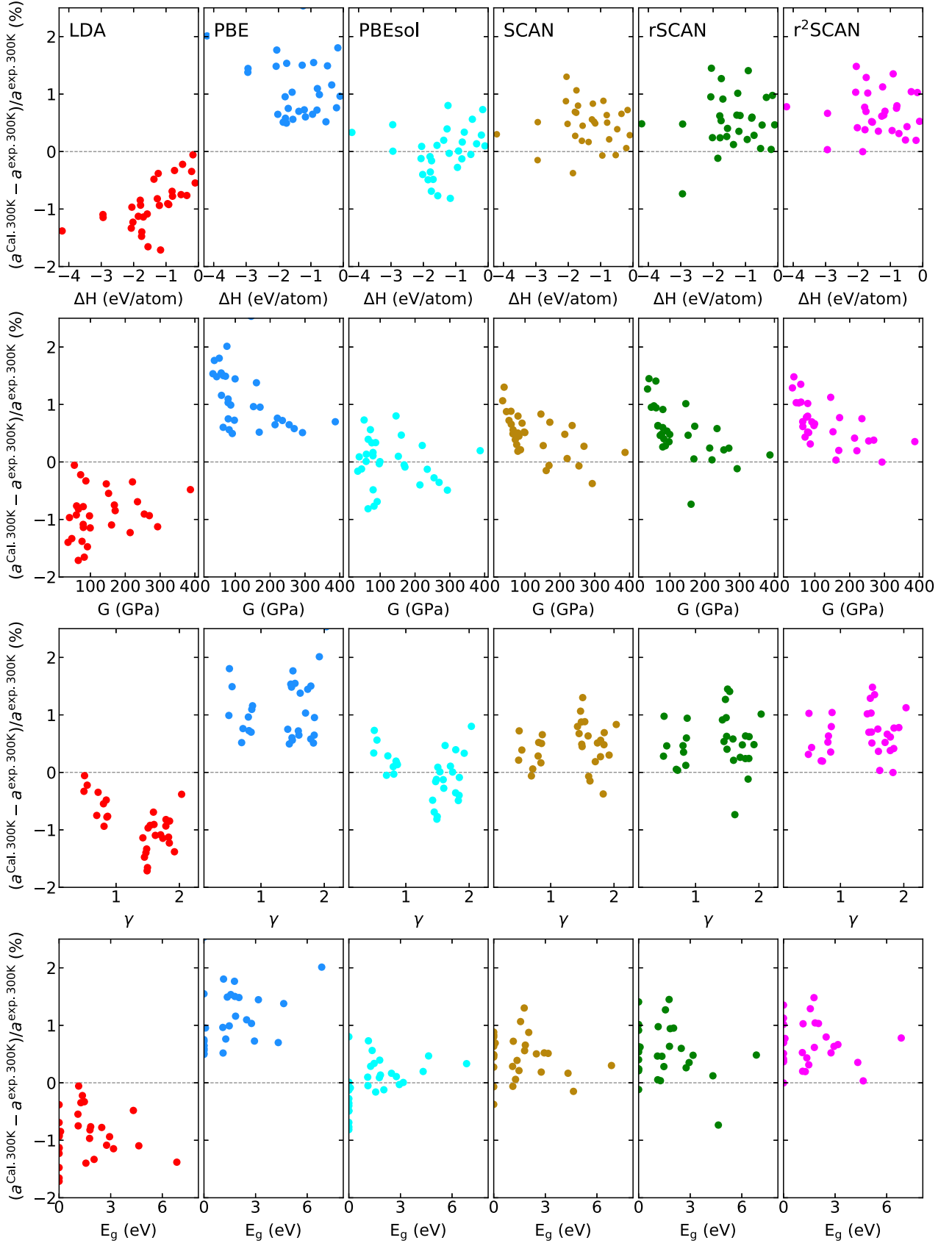


FIG. 4. Correlation between the relative errors of DFT calculated lattice constants at 300 K within the QHA with respect to the experimental values at room temperature and formation energy (ΔH) adapted from the OQMD [71], bulk modulus (G), Grüneisen parameter (γ) at room temperature, and band gaps (E_g) calculated by PBEsol.

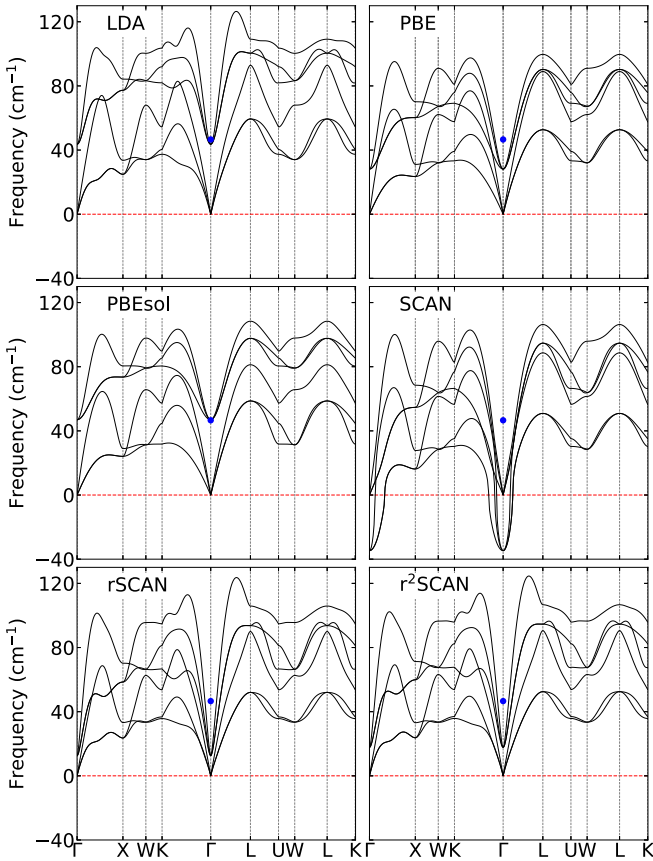


FIG. 5. Phonon spectra of PbTe calculated by LDA, PBE, PBEsol, SCAN, rSCAN, and r²SCAN. The blue circles indicate the Γ_4^- calculated by RPA. Since the RPA forces' calculations are computationally very expensive, we only calculate the phonon at Γ point using the density functional perturbation theory [76]. The negative frequency indicates an imaginary frequency.

of the compounds with poor R^2 (≤ 0.995) are 19 and 7 in the 60-compound dataset for rSCAN and r²SCAN, respectively. We also found that rSCAN has poor R^2 for the compounds without imaginary frequencies, such as GaS, GaSe, ScP, ScBi, but did not find such cases in r²SCAN. Interestingly, these numerical instabilities in the EOS fitting are not observed in LDA, PBE, and PBEsol. Unfortunately, the origin of these numerical instabilities appearing for SCAN, rSCAN, and r²SCAN is unclear to us at present and therefore calls for further study.

F. Unstable phonon modes at the equilibrium volume predicted by SCAN-related functionals

Apart from the imaginary frequencies caused by numerical instabilities, SCAN-related functionals even predict that several compounds have imaginary frequencies at their equilibrium volumes, indicating a structural phase transition. For example, SCAN predicts PbTe to have an unstable phonon mode at the Γ point (see Fig. 5), and rSCAN predicts an imaginary frequency at the M point for YCu. In the following, we take PbTe as a representative example and discuss it in more detail. Since the primitive unit cell of PbTe has only two atoms, both the acoustic and optical phonon modes at the Γ

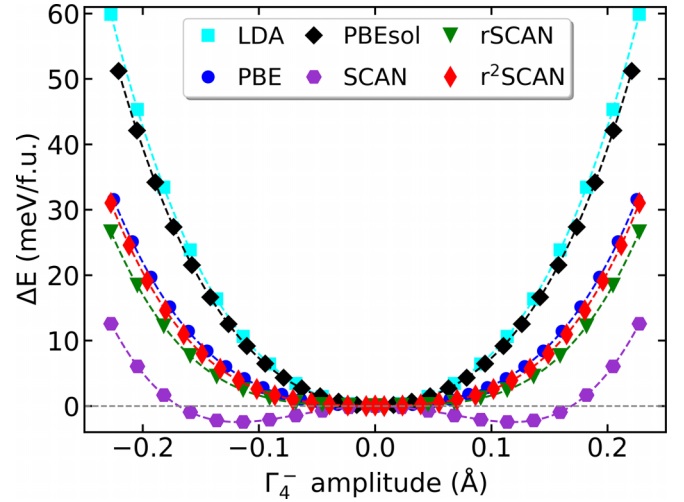


FIG. 6. Energy difference (ΔE) as a function of the structure distortion amplitude of Γ_4^- mode along the [111] direction of cubic PbTe calculated by LDA, PBE, PBEsol, SCAN, rSCAN, and r²SCAN.

point have T_{1u} symmetry (labeled as Γ_4^-), and the optical one represents the displacement of Pb and Te atoms in opposite directions. For all the studied functionals, only SCAN calculated phonon exhibits an unstable ($\omega^2 < 0$, $\omega = -39.4i$ cm^{-1}) mode at the Γ point, indicating that the rocksalt PbTe is dynamically unstable at 0 K predicted by SCAN and would experience a structural phase transition at a low temperature. This is in contrast to experimental observations, results from the other five functionals, as well as the previous calculations [44,72,73]. Although all other functionals do not predict unstable mode Γ_4^- , we do find that its frequency is very sensitive to the specific exchange-correlation functional. Usually, phonon frequencies are strongly dependent on bond strength (bond length): the stronger bond interaction leads to a larger phonon frequency, and vice versa. Indeed, the phonon frequencies predicted by SCAN are larger than PBE except Γ_4^- , which is a unique characteristic of PbTe-like compounds and is related to the low lattice thermal conductivity [74]. It was found that this phonon mode is even much more sensitive to the bond length of Pb-Te, and a longer bond leads to remarkable phonon softening [75]. However, it is quite surprising that SCAN, which yields a shorter Pb-Te bond length (3.24 Å) than PBE (3.28 Å), predicts a much softer Γ_4^- than PBE. This implies that SCAN has some issues in describing this phonon mode in PbTe. Although the frequencies of Γ_4^- calculated by rSCAN ($\omega = 12.6$ cm^{-1}) and r²SCAN ($\omega = 17.8$ cm^{-1}) are positive, they are still far below than the value calculated by more accurate many-body RPA ($\omega = 46.6$ cm^{-1}). By contrast, the other three functionals have much closer frequencies as compared to RPA. In particular, the PBEsol functional achieves a perfect agreement with RPA (see Fig. 5).

The presence of an unstable ferroelectric phonon mode implies that there might be a ferroelectric phase transition driven by this soft mode below the critical temperature T_c . Therefore, we condensed the unstable Γ_4^- phonon mode by displacing the atoms of the rocksalt PbTe following its eigenvectors of force constant matrix. The subgroups of $Fm\bar{3}m$ connected by Γ_4^- are $I4mm$, $Imm2$, and $R3m$ along [001], [110], and [111]

directions, respectively. We find that $R3m$ has the largest energy gain (~ 3 meV/f.u.) with respect to $Fm\bar{3}m$ calculated by SCAN. Note that the $R3m$ phase is experimentally observed in GeTe and SnTe below T_c , but not in PbTe. In Fig. 6, we show the calculated potential energy surfaces of PbTe along the [111] direction of Γ_4^- mode for SCAN and other functionals. According to the SCAN prediction, the ferroelectric phase $R3m$ can be spontaneously established by gaining energy due to the presence of the double well potential. Although the energy gain is small, the structure distortion (~ 0.11 Å) is quite large. The small energy gain in PbTe arises from the weak bonding interaction. With Pb and Te atoms moving oppositely along the [111] direction of the rocksalt lattice, the space group of the high-symmetry phase ($Fm\bar{3}m$) is reduced to $R3m$ and the Pb-Te bond lengths of $PbTe_6$ octahedra are no longer equal: three Pb-Te bonds are shortened and other three are lengthened. The Pb-Te bond lengths difference calculated by SCAN is about 0.256 Å, which should be detectable in experiments. However, no ferroelectric phase transition in PbTe has been experimentally reported, indicating that SCAN predicts a spurious ferroelectric instability in PbTe. On the other hand, this small structure instability associated with the imaginary frequency at the Γ point can be stabilized by zero point energy, which is not included in our phonon calculations. To demonstrate this, we performed phonon renormalization at 0.1 K using the SCAN functional and found that the unstable phonon mode at the Γ point is stabilized (see Fig. S10 [62]).

We observe a similar result in rSCAN, which predicts that YCu has imaginary frequencies at the M point. The imaginary phonon ($M_5^-, \omega = -33i$ cm $^{-1}$) leads to a low-symmetry phase ($Cmmm$) with the energy of 0.2 meV/f.u. lower than the cubic phase. The amplitude of the M_5^- distortion in $Cmmm$ phase is 0.0056 Å and the Y-Cu bonds split into two groups with a difference of 0.00454 Å. However, the other functionals including SCAN do not have this instability issue; see Fig. S9 [62].

IV. CONCLUSIONS

To conclude, we have assessed the performance of three commonly used functionals (LDA, PBE, and PBEsol) in solids and three SCAN-based functionals (SCAN, rSCAN, and r^2 SCAN) on room-temperature lattice constants predictions on an extensive dataset containing 60 cubic binary compounds within the quasiharmonic approximation. Among these functionals, PBEsol turns out to perform best, yielding the smallest mean absolute relative error, which is followed in decreasing order by SCAN, rSCAN, r^2 SCAN, LDA, and PBE. We find that SCAN suffers numerical stability issues. Specifically, 30 compounds either have imaginary phonon modes at some of the 11 volumes or have a bad fitting of the equation of state. Two revised variants of SCAN, i.e., rSCAN and r^2 SCAN, have better numerical stabilities but demonstrate slightly larger lattice constant errors. LDA, PBE, and PBEsol have much better Grüneisen parameter predictions than the SCAN-based functionals. Considering that the SCAN-based functionals are computationally more demanding due to higher cutoff energy and denser FFT grid required and only show limited improvement on anharmonicity, these functionals are therefore not recommended to use in studying anharmonicity properties. The underlying physical mechanisms are worth further investigation.

ACKNOWLEDGMENTS

X.S. and J.H. acknowledge the support of the Fundamental Research Funds for the Central Universities China (USTB). P.L. is supported by the Shenyang National Research Center for Materials Science (No. E21SLA07). Y.X. acknowledges Portland State University's laboratory setup fund. The computing resource was supported by USTB MatCom of Beijing Advanced Innovation Center for Materials Genome Engineering.

-
- [1] D. M. Ceperley and B. J. Alder, *Phys. Rev. Lett.* **45**, 566 (1980).
 - [2] J. P. Perdew, J. A. Chevary, S. H. Vosko, K. A. Jackson, M. R. Pederson, D. J. Singh, and C. Fiolhais, *Phys. Rev. B* **46**, 6671 (1992).
 - [3] J. P. Perdew, K. Burke, and M. Ernzerhof, *Phys. Rev. Lett.* **77**, 3865 (1996).
 - [4] J. P. Perdew and K. Schmidt, *AIP Conf. Proc.* **577**, 1 (2001).
 - [5] J. Tao, J. P. Perdew, V. N. Staroverov, and G. E. Scuseria, *Phys. Rev. Lett.* **91**, 146401 (2003).
 - [6] Y. Zhao and D. G. Truhlar, *J. Chem. Phys.* **125**, 194101 (2006).
 - [7] Y. Zhao and D. G. Truhlar, *Theor. Chem. Acc.* **120**, 215 (2008).
 - [8] A. D. Becke, *J. Chem. Phys.* **98**, 1372 (1993).
 - [9] J. P. Perdew, M. Ernzerhof, and K. Burke, *J. Chem. Phys.* **105**, 9982 (1996).
 - [10] C. Adamo and V. Barone, *J. Chem. Phys.* **110**, 6158 (1999).
 - [11] J. Heyd, G. E. Scuseria, and M. Ernzerhof, *J. Chem. Phys.* **118**, 8207 (2003).
 - [12] E. Bremond, I. Ciofini, J. C. Sancho-García, and C. Adamo, *Acc. Chem. Res.* **49**, 1503 (2016).
 - [13] W. Kohn and L. J. Sham, *Phys. Rev.* **140**, A1133 (1965).
 - [14] J. P. Perdew, A. Ruzsinszky, G. I. Csonka, O. A. Vydrov, G. E. Scuseria, L. A. Constantin, X. Zhou, and K. Burke, *Phys. Rev. Lett.* **100**, 136406 (2008).
 - [15] J. Heyd, J. E. Peralta, G. E. Scuseria, and R. L. Martin, *J. Chem. Phys.* **123**, 174101 (2005).
 - [16] J. He, K. Hummer, and C. Franchini, *Phys. Rev. B* **89**, 075409 (2014).
 - [17] J. Sun, A. Ruzsinszky, and J. P. Perdew, *Phys. Rev. Lett.* **115**, 036402 (2015).
 - [18] J. Sun, R. C. Remsing, Y. Zhang, Z. Sun, A. Ruzsinszky, H. Peng, Z. Yang, A. Paul, U. Waghmare, X. Wu *et al.*, *Nat. Chem.* **8**, 831 (2016).
 - [19] D. A. Kitchaev, H. Peng, Y. Liu, J. Sun, J. P. Perdew, and G. Ceder, *Phys. Rev. B* **93**, 045132 (2016).
 - [20] M. Ekholm, D. Gambino, H. J. M. Jönsson, F. Tasnádi, B. Alling, and I. A. Abrikosov, *Phys. Rev. B* **98**, 094413 (2018).
 - [21] F. Tran, J. Stelzl, and P. Blaha, *J. Chem. Phys.* **144**, 204120 (2016).
 - [22] E. B. Isaacs and C. Wolverton, *Phys. Rev. Mater.* **2**, 063801 (2018).

- [23] Y. Fu and D. J. Singh, *Phys. Rev. Lett.* **121**, 207201 (2018).
- [24] N. Charles and J. M. Rondinelli, *Phys. Rev. B* **94**, 174108 (2016).
- [25] A. P. Bartók and J. R. Yates, *J. Chem. Phys.* **150**, 161101 (2019).
- [26] J. W. Furness, A. D. Kaplan, J. Ning, J. P. Perdew, and J. Sun, *J. Phys. Chem. Lett.* **11**, 8208 (2020).
- [27] D. Mejía-Rodríguez and S. Trickey, *J. Chem. Phys.* **151**, 207101 (2019).
- [28] A. P. Bartók and J. R. Yates, *J. Chem. Phys.* **151**, 207102 (2019).
- [29] R. Kingsbury, A. S. Gupta, C. J. Bartel, J. M. Munro, S. Dwaraknath, M. Horton, and K. A. Persson, *Phys. Rev. Mater.* **6**, 013801 (2022).
- [30] V. N. Staroverov, G. E. Scuseria, J. Tao, and J. P. Perdew, *Phys. Rev. B* **69**, 075102 (2004).
- [31] J. Sun, M. Marsman, G. I. Csonka, A. Ruzsinszky, P. Hao, Y.-S. Kim, G. Kresse, and J. P. Perdew, *Phys. Rev. B* **84**, 035117 (2011).
- [32] G. I. Csonka, J. P. Perdew, A. Ruzsinszky, P. H. T. Philipsen, S. Lebègue, J. Paier, O. A. Vydrov, and J. G. Ángyán, *Phys. Rev. B* **79**, 155107 (2009).
- [33] P. Haas, F. Tran, and P. Blaha, *Phys. Rev. B* **79**, 085104 (2009).
- [34] S. Jana, K. Sharma, and P. Samal, *J. Chem. Phys.* **149**, 164703 (2018).
- [35] L. Schimka, J. Harl, and G. Kresse, *J. Chem. Phys.* **134**, 024116 (2011).
- [36] J. Harl, L. Schimka, and G. Kresse, *Phys. Rev. B* **81**, 115126 (2010).
- [37] G.-X. Zhang, A. M. Reilly, A. Tkatchenko, and M. Scheffler, *New J. Phys.* **20**, 063020 (2018).
- [38] Y. Xia, K. Pal, J. He, V. Ozoliņš, and C. Wolverton, *Phys. Rev. Lett.* **124**, 065901 (2020).
- [39] A. Jain, *Phys. Rev. B* **102**, 201201(R) (2020).
- [40] Y. Oba, T. Tadano, R. Akashi, and S. Tsuneyuki, *Phys. Rev. Mater.* **3**, 033601 (2019).
- [41] S. Bichelmaier, J. Carrete, M. Nelhiebel, and G. K. Madsen, *Phys. Status Solidi RRL* **16**, 2100642 (2022).
- [42] T. Amano, T. Yamazaki, R. Akashi, T. Tadano, and S. Tsuneyuki, *Phys. Rev. B* **107**, 094305 (2023).
- [43] A. Togo, L. Chaput, I. Tanaka, and G. Hug, *Phys. Rev. B* **81**, 174301 (2010).
- [44] J. M. Skelton, D. Tiana, S. C. Parker, A. Togo, I. Tanaka, and A. Walsh, *J. Chem. Phys.* **143**, 064710 (2015).
- [45] J. Linnera, A. Erba, and A. J. Karttunen, *J. Chem. Phys.* **151**, 184109 (2019).
- [46] C. N. Saunders, D. S. Kim, O. Hellman, H. L. Smith, N. J. Weadock, S. T. Omelchenko, G. E. Granroth, C. M. Bernal-Choban, S. H. Lohaus, D. L. Abernathy, and B. Fultz, *Phys. Rev. B* **105**, 174308 (2022).
- [47] Q. Cai, D. Scullion, W. Gan, A. Falin, S. Zhang, K. Watanabe, T. Taniguchi, Y. Chen, E. J. Santos, and L. H. Li, *Sci. Adv.* **5**, eaav0129 (2019).
- [48] S. d'Ambrumenil, M. Zbiri, A. M. Chippindale, and S. J. Hibble, *Phys. Rev. B* **100**, 094312 (2019).
- [49] G. Liu, Z. Gao, and J. Ren, *Phys. Rev. B* **99**, 195436 (2019).
- [50] R. Mittal, M. K. Gupta, B. Singh, L. Pintschovius, Y. D. Zavartsev, and S. L. Chaplot, *Phys. Rev. Mater.* **3**, 043608 (2019).
- [51] P. E. Blöchl, *Phys. Rev. B* **50**, 17953 (1994).
- [52] G. Kresse and D. Joubert, *Phys. Rev. B* **59**, 1758 (1999).
- [53] G. Kresse and J. Hafner, *Phys. Rev. B* **48**, 13115 (1993).
- [54] G. Kresse and J. Furthmüller, *Comput. Mater. Sci.* **6**, 15 (1996).
- [55] F. D. Murnaghan, *Proc. Natl. Acad. Sci. (USA)* **30**, 244 (1944).
- [56] P. Nozières and D. Pines, *Phys. Rev.* **109**, 741 (1958).
- [57] J. Harl and G. Kresse, *Phys. Rev. Lett.* **103**, 056401 (2009).
- [58] M. Bokdam, J. Lahnsteiner, B. Ramberger, T. Schäfer, and G. Kresse, *Phys. Rev. Lett.* **119**, 145501 (2017).
- [59] F. Jia, G. Kresse, C. Franchini, P. Liu, J. Wang, A. Stroppa, and W. Ren, *Phys. Rev. Mater.* **3**, 103801 (2019).
- [60] C. Verdi, L. Ranalli, C. Franchini, and G. Kresse, *Phys. Rev. Mater.* **7**, L030801 (2023).
- [61] L. Ranalli, C. Verdi, L. Monacelli, G. Kresse, M. Calandra, and C. Franchini, *Adv. Quantum Technol.* **6**, 2200131 (2023).
- [62] See Supplemental Material at <http://link.aps.org/supplemental/10.1103/PhysRevB.108.024306> for the imaginary frequency number of each functional, R^2 value for fitting Murnaghan equation, Grüneisen parameters, ZPE correction, RE of lattice constants calculated using ZPE correction and QHA, correlation between RE and physical properties, RE of lattice constants computed at 0 K, compounds with low R^2 for fitting Helmholtz free energy by SCAN, compounds with low R^2 for fitting Helmholtz free energy by rSCAN and r²SCAN, phonon dispersion of YCu, and phonon dispersion of PbTe calculated at 0.1 K by SCAN.
- [63] Y. Zhao and D. G. Truhlar, *J. Chem. Phys.* **128**, 184109 (2008).
- [64] J. Heyd and G. E. Scuseria, *J. Chem. Phys.* **121**, 1187 (2004).
- [65] D. T. Morelli and G. A. Slack, in *High Thermal Conductivity Materials* (Springer, New York, 2006), pp. 37–68.
- [66] D. T. Morelli, J. P. Heremans, and G. A. Slack, *Phys. Rev. B* **66**, 195304 (2002).
- [67] E. T. Ritz, S. J. Li, and N. A. Benedek, *J. Appl. Phys.* **126**, 171102 (2019).
- [68] *High Thermal Conductivity Materials*, edited by S. L. Shindé and J. Goela (Springer, New York, 2006).
- [69] T. Scabarozzi, S. Amini, O. Leaffer, A. Ganguly, S. Gupta, W. Tambussi, S. Clipper, I. J. Spanier, M. Barsoum, J. Hettinger *et al.*, *J. Appl. Phys.* **105**, 013543 (2009).
- [70] R. Roberts and G. White, *J. Phys. C: Solid State Phys.* **19**, 7167 (1986).
- [71] S. Kirklin, J. E. Saal, B. Meredig, A. Thompson, J. W. Doak, M. Aykol, S. Rühl, and C. Wolverton, *npj Comput. Mater.* **1**, 15010 (2015).
- [72] G. A. S. Ribeiro, L. Paulatto, R. Bianco, I. Errea, F. Mauri, and M. Calandra, *Phys. Rev. B* **97**, 014306 (2018).
- [73] Y. Xia, *Appl. Phys. Lett.* **113**, 073901 (2018).
- [74] S. Lee, K. Esfarjani, T. Luo, J. Zhou, Z. Tian, and G. Chen, *Nat. Commun.* **5**, 3525 (2014).
- [75] J. Haeni, P. Irvin, W. Chang, R. Uecker, P. Reiche, Y. Li, S. Choudhury, W. Tian, M. Hawley, B. Craigo *et al.*, *Nature (London)* **430**, 758 (2004).
- [76] S. Baroni, S. de Gironcoli, A. Dal Corso, and P. Giannozzi, *Rev. Mod. Phys.* **73**, 515 (2001).